arXiv:1201.1690v1 [cond-mat.mes-hall] 9 Jan 2012

A topological look at the quantum spin Hall state

Huichao Li, L. Sheng,* and D. Y. Xing
National Laboratory of Solid State Microstructures and Department of Physics, Nanjing University, Nanjing 210093, China

We propose a topological understanding of the quantum spin Hall state without considering any symmetries, and it follows from the gauge invariance that either the energy gap or the spin spectrum gap needs to close on the system edges, the former scenario generally resulting in counterpropagating gapless edge states. Based upon the Kane-Mele model with a uniform exchange field and a sublattice staggered confining potential near the sample boundaries, we demonstrate the existence of such gapless edge states and their robust properties in the presence of impurities. These gapless edge states are protected by the band topology alone, rather than any symmetries.

PACS numbers: 72.25.-b, 73.20.At, 73.22.-f, 73.43.-f

Since the remarkable discovery of the quantum Hall effect (QHE) [1], the study of edge state physics has attracted much attention on both theoretical and experimental sides. Recently, a new class of topological states of matter has emerged, called the quantum spin Hall (QSH) states [2, 3]. A QSH state of matter has a bulk energy gap separating the valence and conduction bands and a pair of spin-filtered gapless edge states on the boundary. The QSH effect was first predicted in two-dimensional (2D) models [2, 3], and was experimentally confirmed soon after in mercury telluride quantum wells [4]. The QSH systems are 2D topological insulators [5, 6] protected by the time-reversal symmetry (TRS), whose edge states are robust against perturbations such as nonmagnetic disorder.

A simple model of the QSH systems is the Kane-Mele model [2], defined on a honeycomb lattice, first introduced for graphene with spin-orbit couplings (SOCs). It was suggested [2] that the intrinsic SOC in graphene would open a band gap in the bulk and also establish spin-filtered edge states that traverse the band gap, giving rise to the QSH effect. Even though the intrinsic SOC strength in pure graphene is too small to produce an observable effect under realistic conditions [7], the Kane-Mele model captures the essential physics of the QSH state with nontrivial band topology [8, 9]. In the presence of the Rashba SOC and an exchange field, the Kane-Mele model enters a TRS-broken QSH phase [10] characterized by nonzero spin Chern numbers [11, 12]. Prodan proved [12] that the spin-Chern numbers are topological invariants, as long as the energy gap and the spectrum gap of the projected spin operator $P\sigma_z P$ stay open in the bulk, where P is the projection operator onto the subspace of the occupied bands and σ_z the Pauli matrix for the electron spin. Unlike the Z_2 invariant [13], the robust properties of the spin-Chern numbers remain unchanged when the TRS is broken [10, 12].

The existence of counterpropagating edge states with opposite spin polarizations is an important characteristic of the QSH state. It is believed that the edge states can be gapless only if the TRS [2] or other symmetries, such as the inversion symmetry [14] or charge-conjugation TRS [15], are present. When the TRS is broken, it was found [10] that a small gap appears in the spectrum of the edge states, which was obtained for a ribbon geometry under ideal boundaries, i.e., boundaries created by an infinite hard-wall confining potential. However, since the edge states are localized around the sample boundaries, they can be sensitive to the variation of on-site potentials near the boundaries [16].

In this Letter, in order to reveal the general characteristics of the edge states and their connection to the bulk topological invariant in a QSH system, we present a topological argument similar to the Laughlin's Gedanken experiment without considering any symmetries. We show that, as required by the nontrivial band topology and gauge invariance, either the energy gap or the spin spectrum gap (the gap in the spectrum of $P\sigma_z P$) needs to close on the edges of a QSH system. These two scenarios will lead to gapless or gapped edge modes, respectively. In particular, it is demonstrated that gapless edge states can appear in a TRS-broken QSH system by tuning the confining potential at the boundaries. They are associated with the bulk topological invariant, and are robust against relatively smooth impurity scattering potential. Our result offers an interesting example for counterpropagating gapless edge states that are not protected by symmetries, which sheds light on the underlying mechanism of the QSH effect in a broad sense.

Let us first look back on a looped ribbon of the QHE system, with a magnetic flux ϕ (in units of flux quantum hc/e) threading the ring adiabatically [17–19]. The Fermi energy E_F is assumed to lie in an energy gap. In the spirit of the Laughlin's argument, increasing ϕ from 0 to 1 effectively pumps one occupied state from one edge to the other, giving rise to the transfer of one charge between the edges, essentially because there is a nonzero Chern number (Hall conductivity) in the bulk. On the other hand, the system Hamiltonian is gauge invariant under integer flux changes, i.e., if ϕ is increased from 0 to 1, the system will reproduce the same eigenstates as at $\phi = 0$. To assure this gauge invariance, there must be gapless edge modes on the edges (when the perimeter of the ring is large), so that the spectral flow can form a closed loop, as illustrated in Fig. 1a, along which the electron states can continuously move with changing ϕ.

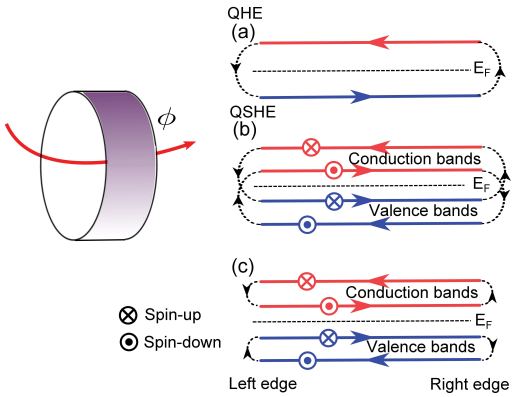

FIG. 1: (a) A schematic of the flow of electron states in a looped ribbon of the QHE system, with adiabatically increasing the magnetic flux ϕ that threads the ring. The bulk electron states below Fermi energy E_F drift from left to right, gapless edge modes ascend through E_F on the right edge, states above E_F drift from right to left, and gapless edge modes descend through E_F on the left edge, forming a closed loop. (b) In the first scenario for the QSH system, gapless edge modes appear on the edges of the ring, so that electron states in each spin sector behave like in the QHE system, but those in two spin sectors move in opposite directions. (c) In the second scenario for the QSH system, the edge states are gapped, whereas the spin spectrum gap closes on the edges. In the bulk, electron states in the two spin sectors drift in the same way as in (b), but on the edges they join together within the valence (conduction) band.

We now propose a topological understanding of the QSH system in terms of the same looped ribbon geometry. The occupied valence band can be decomposed into two spin sectors by using the projected spin operator [10, 12]. (The unoccupied conduction band can be divided similarly.) The two spin sectors are separated by a nonzero spin spectrum gap in the bulk. They carry opposite spin Chern numbers, so that increasing ϕ pumps a state of the spin up sector in the occupied band from one edge to the other, and pumps another state of the spin down sector in the opposite direction. In order for the system to recover the initial eigenstates as ϕ changes from 0 to 1, the spectral flow needs to form closed loops, similarly to the QHE system. However, for the QSH system, if not enforced by any symmetry, two different scenarios can occur on the edges. One is that gapless edge modes appear on the edges, so that states can move between the conduction and valence bands with changing ϕ to form closed loops in the spin-up and spin-down sectors separately, as shown in Fig. 1b. In this case, the states in the two loops cannot evolve into each other due to the nonvanishing spin spectrum gap both in the bulk and on the edges. The other scenario is that a closed loop of spectral flow is formed between the two spin sectors within the valence (or conduction) band, as shown in Fig. 1c. In this case, the spin spectrum gap must vanish on the edges, but the energy gap may remain open in the edge state spectrum.

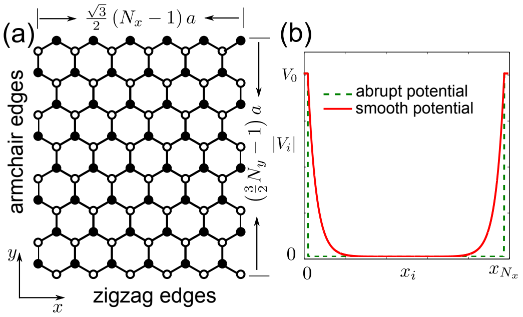

FIG. 2: (a) A schematic of an armchair honeycomb lattice ribbon with atom sites in two sublattices being labeled by solid dots and hollow dots, where a is the distance between nearest-neighbor sites. (b) Profiles of $|V_i|$ as functions of x_i, for an abrupt confining potential (dashed line) and a relatively smooth confining potential (solid line).

The above topological discussion on the QSH system is very general, independent of any symmetries. To demonstrate the two scenarios in Figs. 1b and 1c, in what follows we take the Kane-Mele model [2] for a honeycomb lattice ribbon as an example, by taking into account different confining potentials near the edges of the ribbon. It was shown that in a suitable parameter range, the Kane-Mele system is in the QSH phase protected by the TRS, and it can become a TRS-broken QSH phase [10], when a spin-splitting exchange field is applied. Consider an armchair ribbon along the y direction, as shown in Fig. 2a, including N_x dimer lines across the ribbon. (Results for a zigzag ribbon are similar.) The boundaries are at $x_1 = 0$ and $x_{N_x} = \frac{\sqrt{3}}{2}(N_x - 1)$, where the distance between nearest-neighbor sites is chosen as the unit of length. The Hamiltonian can be written as $H = H_{KM} + H_E + H_C$ with

$$\begin{aligned} H_{KM} &= -t\sum_{\langle ij\rangle} c_i^\dagger c_j + \frac{2i}{\sqrt{3}} V_{SO} \sum_{\langle\langle ij\rangle\rangle} c_i^\dagger \boldsymbol{\sigma}\cdot(\boldsymbol{d}_{kj}\times\boldsymbol{d}_{ik})c_j \\ &+ iV_R\sum_{\langle ij\rangle} c_i^\dagger \hat{\boldsymbol{e}}_z\cdot(\boldsymbol{\sigma}\times\boldsymbol{d}_{ij})c_j, \end{aligned} \tag{1}$$

as the Hamiltonian of the Kane-Mele model. Here, the first term is the nearest-neighbor hopping term with $c_i^\dagger = (c_{i\uparrow}^\dagger, c_{i\downarrow}^\dagger)$ as the electron creation operator on site i and the angular bracket in $\langle i,j\rangle$ standing for nearest-neighbor sites. The second term is the intrinsic SOC with coupling strength V_{SO}, where $\boldsymbol{\sigma}$ are the Pauli matrices, i and j are two next nearest neighbor sites, k is their unique common nearest neighbor, and vector $\mathbf{d}_{ik}$ points from k to i. The third term is the Rashba SOC with coupling strength V_R. $H_E = g\sum_i c_i^\dagger\sigma_z c_i$ stands for a uniform exchange field of strength g. H_C represents a sublattice staggered confining potential, which is given by $H_C = \sum_i V_i c_i^\dagger c_i$ with

$$V_i = \pm V_0 \left(e^{-\frac{x_i}{\xi}} + e^{-\frac{x_{N_x} - x_i}{\xi}} \right) , \qquad (2)$$

where ± is taken to be positive for sites on sublattice A (solid dots) and negative on sublattice B (hollow dots), as shown in the Fig. 2a. In Eq. (2), V_i is strongly x dependent across the ribbon, equal to $\pm V_0$ at the edges ($x_i = 0$ and $x_i = x_{N_x}$). It decays exponentially away from the edges, with a characteristic length ξ, as shown in Fig. 2b. When the ribbon width is much greater than ξ, V_i essentially vanishes in the middle region of the ribbon. Here, we note that in the case of a uniform staggered potential $V_i = \pm V_0$ ($|V_i|$ being independent of x_i), it was shown [10] that with increasing $|V_i|$, there is a transition from the TRS-broken QSH phase to an ordinary insulator state, where the middle band gap closes and then reopens. Therefore, for the confining potential V_i given by Eq. (2) with large V_0, the ribbon in Fig. 2 can be regarded as a TRS-broken QSH ribbon sandwiched in between two trivial band insulators.

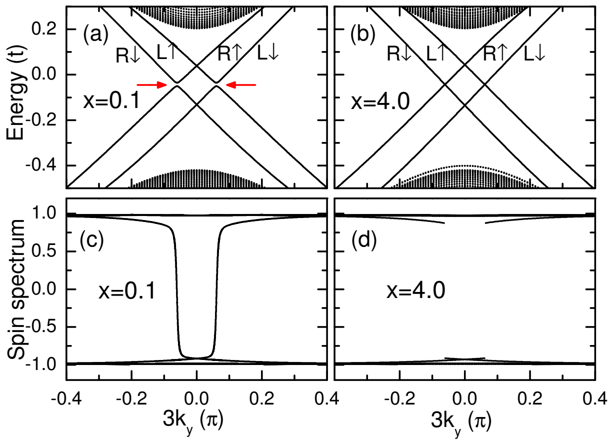

FIG. 3: (color online) The energy spectrum (a, b) and the spectrum of the projected spin $P\sigma_z P$ (c, d) of an armchair ribbon for $\xi = 0.1$ (a, c) and $\xi = 4$ (b, d), in which L (R) stands for states on the left (right) edge, and ↑ (↓) for the up (down) spin polarization. The horizontal arrows in (a) point to the small energy gaps in the energy spectrum. At $\xi = 0.1$, while the energy spectrum (a) is gapped, the spin spectrum (c) is gapless. At $\xi = 4$, the energy spectrum (b) is gapless, but the spin spectrum (d) is gapped.

In order to assure the system in the TRS-broken QSH state, we set the parameters $V_{so} = 0.1t$, $V_R = 0.1t$, and $g = 0.1t$. The length of the armchair ribbon N_y is taken to be infinite. The energy spectrum of the ribbon, together with the corresponding eigenfunctions $\varphi_m(k_y)$, can be numerically obtained by diagonalizing the Hamiltonian for each momentum k_y in the y direction. The calculated energy spectrum of the armchair ribbon with width $N_x = 240$, for the confining potential with $V_0 = 12t$ fixed and two different decay lengths, is plotted in Fig. 3a and Fig. 3b. One can see easily that the edge states appear as thin lines in the middle bulk band gap of the energy spectrum. In Figs. 3a and 3b, the spin polarization of the edge states is labeled with ↑ and ↓, indicating that two spin-filtered channels on each edge flow along opposite directions. For the nearly hard-wall confining potential of $\xi = 0.1$, the sublattice potential V_i is nonzero only on the outermost armchair lines, similar to the assumption in Ref. [16]. In this case, two small energy gaps are observed in the edge state spectrum shown in Fig. 3a, in agreement with the previous observation [10], as a consequence of the broken TRS. With increasing the decay length ξ of the confining potential, the energy gaps of the edge states become smaller and smaller. As ξ is large enough, e.g., $\xi = 4$ in Fig. 3b, interestingly, the edge states become gapless.

We now calculate the k_y-dependent spectrum of projected spin operator $P\sigma_z P$, whose matrix elements are given by $\langle \varphi_m(k_y) | \sigma_z | \varphi_n(k_y) \rangle$ with m and n running over all the occupied states. By diagonalizing this matrix, the spectrum of the projected spin $P\sigma_z P$ can be obtained. For the Kane-Mele model Eq. (1), if $V_R = 0$, σ_z commutes with the Hamiltonian H. Therefore, σ_z is a good quantum number. It follows that the spectrum of $P\sigma_z P$ consists of just two values ±1, which are highly degenerate. When the Rashba term is turned on, σ_z and H no longer commute, and the degeneracy is lifted. In this case, the spectra of $P\sigma_z P$ between $+1$ and -1 spread towards the origin, but a gap remains for a bulk sample if the amplitude of the Rashba term dose not exceed a threshold [12].

For the ribbon geometry, the situation is more complicated due to the existence of the edges, and numerical calculations are performed to obtain the spin spectrum. The calculated spectrum of $P\sigma_z P$ for the same parameters as those in Figs. 3a and 3b is shown in Figs. 3c and 3d, which exhibits very interesting behavior. For the hard-wall confining potential with $\xi = 0.1$, while the energy spectrum of edge states are slightly gapped, with increasing k_y the spectrum of $P\sigma_z P$ continuously change between $+1$ to -1 without showing any gap, corresponding to the second scenario shown in Fig. 1c. On the other hand, for a relatively smooth confining potential with $\xi = 4.0$, the energy spectrum of the edge states are gapless, but the spectrum of $P\sigma_z P$ displays a big gap, and the sudden changes happen at the cross points in the energy spectrum of the edge states, corresponding to the first scenario shown in Fig. 1b. From Fig. 3, it follows that as long as the system is in the QSH state, a gapless characteristic always appears either in the energy spectrum of edge states or in the spectrum of $P\sigma_z P$, leading to the two types of closed loops for the continuous flow of the electron states illustrated in Figs. (1b, 1c).

The result shown in Figs. 3b and 3d, for the relatively smooth confining potential, is of particular interest. It indicates that gapless edge states can exist in the TRS-broken QSH system, accompanied with a gapped spectrum of $P\sigma_z P$. Such an interesting behavior can be further understood by the following argument. As long as the bulk energy gap does not close, the projected spin operator $P\sigma_z P$ is exponentially localized in real space with a characteristic length about $\lambda \sim \hbar v_F / \Delta_E$, where v_F is the Fermi velocity and Δ_E is the magnitude of the energy gap. [12] For the parameter set used in Fig. 3, λ is estimated to be between 1 to 2 lattice constants. When the confining potential V_i is varying relatively slowly in space, i.e., $\xi \gg \lambda$, one can find that $P\sigma_z P$ roughly commutes with the confining potential. In this case, the confining potential is of no influence on the spectrum of $P\sigma_z P$. Since the spin spectrum has a gap in the bulk [10], this gap remains to open on the smooth edges, as seen from Fig. 3d. As a result, the energy gap has to close due to the topological requirement, resulting in gapless edge modes, as observed in Fig. 3b.

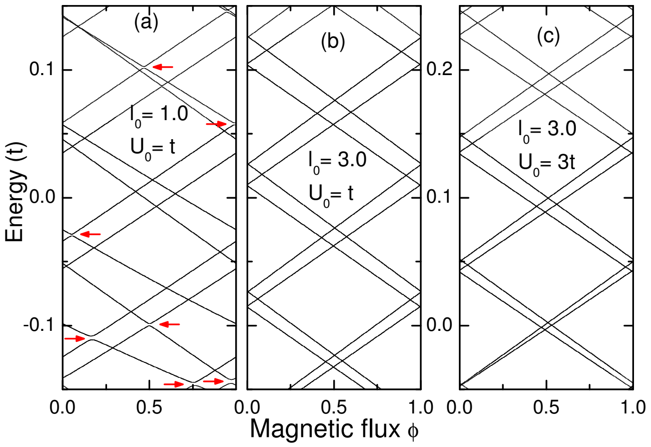

FIG. 4: (color online) Eigenenergies of the edge states as a function of the magnetic flux ϕ threading the looped geometry with size 120×60 for (a) $l_0 = 1.0$, $U_0 = t$, (b) $l_0 = 3.0$, $U_0 = t$, and (c) $l_0 = 3.0$, $U_0 = 3t$, where the impurity concentration is fixed at 1%. The other parameters are taken to be $V_{SO} = V_R = g = 0.1t$, $V_0 = 12t$, and $\xi = 4$. Arrows in (a) indicate some of the relatively large energy gaps.

Finally, we wish to discuss the robustness of the gapless edge states found in the present TRS-broken QSH system. We consider a $N_x \times N_y$ sample forming a looped geometry as that shown in Fig. 1. N_I nonmagnetic impurities are assumed to be randomly distributed in the sample at positions $\mathbf{R}_\alpha$ with $\alpha = 1, \cdots N_I$. An extra term $H_I = \sum_i w_i c_i^\dagger c_i$ is added to the total Hamiltonian H to describe the effect of the impurity scattering, where $w_i = \sum_\alpha U(\mathbf{r}_i - \mathbf{R}_\alpha)$ with $\mathbf{r}_i$ as the position of the i-th atom site. The impurity scattering potential is taken to be $U(\mathbf{r}_i - \mathbf{R}_\alpha) = (U_0/l_0^2) \exp(-|\mathbf{r}_i - \mathbf{R}_\alpha|/l_0)$ with l_0 as the correlation length and U_0 the strength of the scattering potential. By inclusion of $1/l_0^2$ in the prefactor, the area integral of the impurity potential is set to be independent of l_0. Figure 4 shows the evolution of the calculated eigenenergies of a 120×60 system in the band gap upon adiabatic insertion of a magnetic flux ϕ into the ring, for three different impurity scattering potentials. The number concentration of the impurities is fixed at 1%. For a very short correlation length $l_0 = 1$, for which the impurity potential is nearly uncorrelated from one site to another, we see from Fig. 4a that at $U_0 = t$, the energy levels of the edge states avoid to cross each other as they move close, resulting in small energy gaps in the spectrum, as indicated by the arrows. This level repulsion behavior is a signature of the onset of backward scattering [11]. When the characteristic length l_0 is increased to $l_0 = 3$ with $U_0 = t$ fixed, corresponding to a relatively smooth impurity scattering potential, all the energy gaps vanish, as shown in Fig. 4b. The energy levels move in straight lines and continue to cross each other, a clear indication of quenching of the backward scattering [11]. Such a level crossing feature is intact when U_0 is increased up to $3t$ for fixed $l_0 = 3$, as shown in Fig. 4c. We thus conclude that the edge states remain to be robust in the presence of relatively smooth impurity scattering potential of intermediate strength. This result can be understood based upon an argument similar to that in the pure case. When l_0 is greater than the characteristic length λ of the projected spin operator $P\sigma_z P$, the impurity scattering potential nearly commutes with $P\sigma_z P$, and hence does not affect much the spin spectrum gap, so that the energy gap needs to close on the edges, which explains the level crossing behavior of the edge modes.

In summary, based upon a general topological argument without relying on the TRS or other symmetries, we show that in a QSH system either the energy gap or the gap in the spectrum of $P\sigma_z P$ needs to close on the edges. We find that a TRS-broken QSH system can have either gapless or gapped edge states, depending on the properties of the confining potential near the boundaries. The gapless edge states are protected by the bulk topological invariant rather than any symmetries, which can remain to be robust in the presence of impurities.

Acknowledgment This work is supported by the State Key Program for Basic Researches of China under Grant Nos. 2009CB929504 (LS), 2011CB922103 and 2010CB923400 (DYX), by the National Natural Science Foundation of China under Grant Nos. 11074110 (LS), 11174125, 11074109, and 91021003 (DYX), and by a project funded by the PAPD of Jiangsu Higher Education Institutions.

---

* Electronic address: shengli@nju.edu.cn

[1] K. V. Klitzing, G. Dorda, and M. Pepper, Phys. Rev. Lett. **45**, 494 (1980).
[2] C. L. Kane and E. J. Mele, Phys. Rev. Lett. **95**, 226801 (2005).

[3] B. A. Bernevig, T. L. Hughes and S. C. Zhang, Science, **314** 1757 (2006).

[4] M. König, S. Wiedmann, C. Bruene, A. Roth, H. Buhmann, L. W. Molenkamp, X. L. Qi and S. C. Zhang, Science **318**, 766 (2007).

[5] J. E. Moore and L. Balents, Phys. Rev. B, 75, 121306 (2007).

[6] L. Fu, C. L. Kane, and E. J. Mele, Phys. Rev. Lett. 98, 106803 (2007); L. Fu and C. L. Kane, Phys. Rev. B 76, 045302 (2007).

[7] H. Min, J. E. Hill, N. A. Sinitsyn, B. R. Sahu, L. Kleinman, and A. H. MacDonald, Phys. Rev. B **74**, 165310 (2006); Y. Yao, F. Ye, X. L. Qi, S. C. Zhang, and Z. Fang, Phys. Rev. B **75**, 041401(R) (2007).

[8] M. Z. Hasan and C. L. Kane, Rev. Mod. Phys. **82**, 3045 (2010).

[9] X. L. Qi and S. C. Zhang, Rev. Mod. Phys. **83**, 1057 (2011).

[10] Y. Y. Yang, Z. Xu, L. Sheng, B. G. Wang, D. Y. Xing, and D. N. Sheng, Phys. Rev. Lett. **107**, 066602 (2011).

[11] D. N. Sheng, Z. Y. Weng, L. Sheng, and F. D. M. Haldane, Phys. Rev. Lett. **97**, 036808 (2006); L. Sheng, D. N. Sheng, C. S. Ting, and F. D. M. Haldane, Phys. Rev. Lett. **95**, 136602 (2005).

[12] E. Prodan, Phys. Rev. B **80**, 125327 (2009).

[13] C. L. Kane, and E. J. Mele, Phys. Rev. Lett. **95**, 146802 (2005).

[14] B. Zhou, H.-Z. Lu, R.-L. Chu, S.-Q. Shen, and Q. Niu, Phys. Rev. Lett. 101, 246807 (2008).

[15] Q. F. Sun, and X. C. Xie, Phys. Rev. Lett. **104**, 066805 (2010).

[16] W. Yao, S. A. Yang, and Q. Niu, Phys. Rev. Lett. **102**, 096801 (2009).

[17] R. B. Laughlin, Phys. Rev. B **23**, 5632 (1981).

[18] B. I. Halperin, Phys. Rev. B **25**, 2185 (1982).

[19] J. E. Avron, D. Osadchy, and R. Seiler, Physics Today, August (2003), page 38.